

# One-Step Electrochemically Deposited Gold Nanoparticles Interface Grafted with Avidin for Acetylcholinesterase Biosensor Design

Weiyang Zhang, Jiawang Ding, Yuehua Qin, Deli Liu\*, and Dan Du\*

Key Laboratory of Pesticide and Chemical Biology of Ministry of Education,  
Central China Normal University, Wuhan 430079, P. R. China

In this study, an interface embedded *in situ* gold nanoparticles (AuNPs) and biotin in chitosan hydrogel was constructed by one-step electrochemical deposition in solution containing tetrachloroauric (III) acid, biotin and chitosan. This deposited interface acts as biosensing platforms and provides specific binding sites for avidin, which are further capable of attaching any biotinylated bimolecular for biosensor design. Atomic force microscopy (AFM), A.C. impedance and surface plasmon resonance were used to characterize this interface. The immobilized acetylcholinesterase (AChE), as a model, showed excellent activity to its substrate and provided a quantitative measurement of organophosphate pesticide. Under the optimal experimental conditions, the inhibition of dimethoate was proportional to its concentrations in the range of 0.05 to 15  $\mu\text{g mL}^{-1}$  with detection limit of 0.001  $\mu\text{g mL}^{-1}$ . The simple method showed good fabrication reproducibility and acceptable stability, which provided a new avenue for electrochemical biosensor design.

**Keywords:** Electrodeposition, Gold Nanoparticles, Biotin Labeled Acetylcholinesterase, Dimethoate, Biosensor.

## 1. INTRODUCTION

Surfaces grafted with biomolecules have received extensive attention for possible applications in advanced technologies including drug deliver,<sup>1</sup> bioseparation,<sup>2</sup> microreactor,<sup>3</sup> and biosensor fabrication.<sup>4–6</sup> The development of procedures allowing the spatially controlled deposition of biomolecules is especially crucial for tailoring molecular recognition events at surfaces in biosensing as well as for investigating biological interactions.<sup>7,8</sup> Usual methods including direct physical adsorption,<sup>9</sup> encapsulation,<sup>10</sup> cross-linking,<sup>11</sup> and covalent binding<sup>12</sup> have been widely used in biosensor design. In order to create molecular interactions with exigent control of biomolecules at the surface, many new methods have been developed.

Electrochemical deposition has been reported recently as an effective method for immobilization of biomolecules due to the formation of sol-gel films.<sup>13</sup> Compared with the traditional process, electrochemical deposition is simple, the performance conditions are moderate, and it is suitable for selective deposition of films with

controllable thickness.<sup>14</sup> Chitosan as a kind of matrix for biomolecules possess attractive properties including excellent film-forming ability, high permeability toward water, good adhesion, non-toxicity, and biocompatibility.<sup>15</sup> It is one of preferred materials in biosensor design. Previous study indicated that chitosan could be electrodeposited onto gold surface at an initial potential of  $-3.0\text{ V}$ .<sup>16–18</sup> The deposition procedure of chitosan is based on a local electrochemically induced pH modulation caused by the oxidation or reduction of water which can be easily confined to a defined volume at the electrode surface by proper adjustment of the nature, strength, and capacity of the buffer in the electrolyte solution.<sup>19</sup> Incorporation of gold nanoparticles (AuNPs) into polymer matrices has also attracted increasing interest in improving the stability and biocompatibility of interface and enhancing the surface capability for immobilization of biomolecules due to the superior properties of nanoparticles.<sup>20,21</sup> AuNPs embedded in chitosan composite film has been reported<sup>22–24</sup> and the interface embedded AuNPs *in situ* has also been constructed by one-step electrochemical deposition.<sup>25</sup>

Avidin is a glycoprotein (molecular weight, 68 000) found in egg white and is known to contain four identical binding sites to biotin. The binding constant between

\*Authors to whom correspondence should be addressed.

avidin and biotin has been reported to be ca.  $10^{15} \text{ M}^{-1}$ .<sup>26</sup> In this article, the strong affinity between biotin and avidin was used for biosensor fabrication.

Acetylcholinesterase, an enzyme that plays a key role as a neurotransmitter in the central nervous system, was chosen for its high biological (Alzheimer disease<sup>27</sup>) and analytical interest (development of pesticide biosensors.<sup>28, 29</sup> In this study, an interface of biotin in chitosan hydrogel embedded AuNPs *in situ* was constructed by one-step electrochemical deposition. This deposited interface provided specific binding sites for avidin, which was further capable of attaching any biotinylated bimolecular. The immobilized AChE, as a model, showed excellent activity to its substrate and provided a quantitative measurement of organophosphate pesticide.

## 2. MATERIALS AND METHODS

### 2.1. Reagents

Acetylcholinesterase (Type C3389, 500 U/mg from electric eel), acetylthiocholine chloride (ATCl), Sulfosuccinimidyl-6-(biotinamido) hexanoate (NHS-LC-biotin), and avidin (from egg white) were purchased from Sigma-Aldrich (St. Louis, MO, USA) and used as received.  $\text{HAuCl}_4 \cdot 4\text{H}_2\text{O}$  (Au% > 48%) was obtained from TreeChem.co (Shanghai, China). 5, 5'-bithiobis-2-nitrobenzoate (DTNB) was obtained from Alfa Aesar, Dimethoate was obtained from AccuStandard (New Haven, CT, USA). Chitosan (95% deacetylation), phosphate buffer solution (PBS, pH 7.0) and other reagents used were of analytical reagent grade. All aqueous solution was prepared with double distilled water.

### 2.2. Instrumentation

Electrochemical measurements were performed with a CHI 660 c electrochemical workstation. A conventional three-electrode electrochemical cell was used consisting one of the above electrodes, a Pt-wire auxiliary electrode, and an Ag/AgCl reference electrode. The A.C. impedance experiment was carried out in  $5 \text{ mM Fe}(\text{CN})_6^{4-/3-}$  with frequencies ranging from 100 kHz to 0.1 Hz with an amplitude of 5 mV. UV spectra were recorded using a UV-2501 spectrophotometer (Shimadzu, Kyoto, Japan). Atomic force microscopy (AFM) experiments were performed on SPA-300 HV atomic force microscopy with a SPI 3800 controller (Seiko, Japan). The diameter size of gold nanoparticles was measured using Malvern Nano-ZS ZEN3600 (Malvern, UK).

Surface plasmon resonance (SPR) measurements were conducted using a single-channel Autolab SPRINGLE instrument (Eco Chemie, Netherlands). The configuration of this equipment is described elsewhere.<sup>30</sup>

### 2.3. Enzyme Labeling

AChE was labeled to NHS-LC-biotin (AChE-biotin) as following: 0.45 mg NHS-LC-biotin was dissolved in 1 mL of 0.1 M PBS (pH 7.0) containing 0.15 mg AChE. After incubation at 37 °C for 3 h, the excess NHS-LC-biotin was removed via dialysis at 4 °C for 2 days with 0.1 M PBS. The phosphate buffer was replaced every 8 h. The dialysis cassette (Pierce) with molecular weight cutoff of 5000 was used throughout. The activity of the enzyme after biotinylation was determined by the result of acetylthiocholine hydrolysis to thiocholine and the oxidation of 5, 5'-bithiobis-2-nitrobenzoate (DTNB) to yield the yellow 5-thio-2-nitrobenzoic acid, which was detected spectrophotometrically.<sup>31</sup>

### 2.4. Biosensor Design

Gold disk electrode (1.0 mm in diameter) was used for the electrochemical measurement. Before modification, the gold electrode was abraded with fine SiC paper, lightly polished with  $0.05 \mu\text{m}$  alumina, followed by sonication in ethanol and double distilled water for 10 min, respectively.

For electrochemical deposition, a clean gold electrode was immersed in 2.0 mL 0.025% (w/v) chitosan solution including 0.01% (v/v)  $\text{HAuCl}_4 \cdot 4\text{H}_2\text{O}$  and 0.18 mg/mL NHS-LC-biotin and an initial potential  $-3.0 \text{ V}$  was applied on the electrode. The electrodeposition was performed on a CHI 660 C electrochemical workstation. At this potential,  $\text{H}^+$  was reduced to  $\text{H}_2$  at the cathode and released, and the pH near the cathode surface gradually increased. When the pH was higher than 6.3, chitosan became insoluble.<sup>32</sup> After being immersed in PBS 7.0 for one minute to reduce nonspecific interaction, the deposited electrode (biotin-CS-AuNPs/Au) was dried in air at room temperature for about 1 h. After that, the electrode was immersed into 0.01 mg/mL avidin solution for about 30 min and washed by double distilled water. For biosensor design, the electrode was then incubated in AChE-biotin solution for another 2 h to obtain the AChE-biotin-avidin-biotin-CS-AuNPs/Au.

### 2.5. Electrochemical Detection of Pesticide

For the measurements of dimethoate, the pretreated AChE-biotin-avidin-biotin-CS-AuNPs/Au was first immersed in the PBS solution containing different concentrations of standard dimethoate solution for 12 min, and then transferred to the electrochemical cell of 1.0 mL pH 7.0 PBS containing 0.3 mM ATCl to study the electrochemical response by cyclic voltammetry (CV). The inhibition of dimethoate was calculated as follows:

Inhibition (%) =  $100\% \times (i_{\text{P, control}} - i_{\text{P, exp}})/i_{\text{P, control}}$   
Where  $i_{\text{P, control}}$  and  $i_{\text{P, exp}}$  were the peak currents of ATCl on AChE-biotin-avidin-biotin-CS-AuNPs/Au without and with pesticide inhibition, respectively.

### 3. RESULTS AND DISCUSSION

#### 3.1. UV-Vis Spectrum

The position of Soret absorption band can provide detailed information about conformation of protein.<sup>33</sup> Figure 1 shows the UV-vis spectra of biotin, AChE and AChE-biotin. No Soret band was observed in NHS-LC-biotin (curve (a)). However, solution-phase AChE displayed a narrow Soret band at 406 nm (curve (b)). After AChE was labeled to NHS-LC-biotin, an obvious Soret band without shift compared to AChE was clearly seen (curve (c)), indicating that AChE was labeled onto NHS-LC-biotin and no significant denaturation occurred.

Inset in Figure 1 further illustrated the photograph images of the AChE before (2) and after (1) biotinylation in the presence of 5, 5'-bithiobis-2-nitrobenzoate (DTNB) and ATCl. As compared with control experiment (3), the solution was orange. It can be concluded that the enzyme maintains its activity. The activity of the enzyme after biotinylation was determined by acetylthiocholine hydrolysis to thiocholine and the oxidation of DTNB to yield the yellow 5-thio-2-nitrobenzoic acid, which was detected spectrophotometrically at 412 nm.<sup>31</sup> The enzyme after biotinylation maintained 80.2% of its original activity. On the basis of the previous results, we might conclude that the as-prepared AChE-biotin, as a model, could be preliminarily applied for further construction of biosensor.

#### 3.2. AuNPs Characterization

Our previous report has shown that the freshly prepared AuNPs showed a maximum absorbance ( $\lambda_{\max}$ ) at

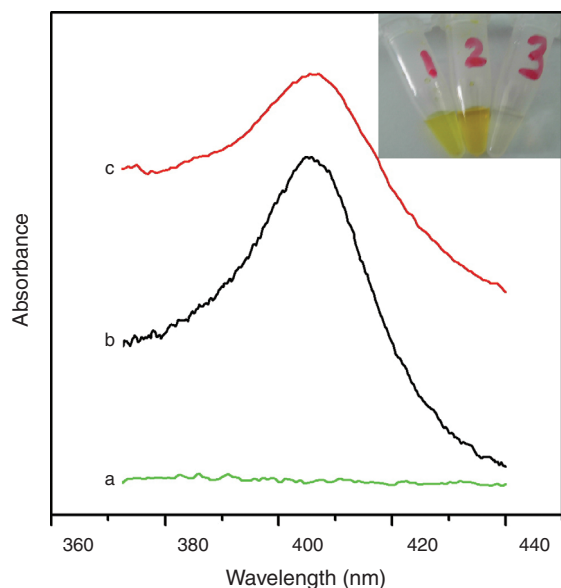


**Fig. 1.** UV spectra of (a) biotin, (b) AChE and (c) biotin-AChE. Inset: photograph images of the AChE before (2) and after (1) biotinylation and control (3) in the absence of 5, 5'-bithiobis-2-nitrobenzoate (DTNB) and ATCl.

524 nm, which was the characteristic absorbance of unaggregated colloidal gold nanoparticles.<sup>25</sup> The laser light scattering measurement has been proven very sensitive to the size, and spatial distribution of metallic nanoparticles. The diameter size of AuNPs was further measured using Malvern Nano-ZS ZEN3600. The average diameter of AuNPs was estimated to be 33 nm (Fig. 2). No agglomeration could be identified even after 3 months.

#### 3.3. AFM Characterization

AFM measurement is an effective method to observe surface topography and confirm the fabrication process. As seen from Figure 3(a), the pretreated bare Au slice displayed an even surface with height less than 1 nm. When the Au slice was immersed in deposition solution containing chitosan,  $\text{HAuCl}_4 \cdot 4\text{H}_2\text{O}$  and NHS-LC-biotin for 2 min, the deposited biotin-CS-AuNPs interface showed a uniform distribution and the embedded biotin in chitosan hydrogel could be clearly seen (Fig. 3(b)). Upon incubation of avidin, Figure 3(c) clearly illustrated that a homogeneous dispersion of avidin was achieved on the biotin-CS-AuNPs interface due to the strong affinity between biotin and avidin. The thickness of all the layers increased to  $\sim 5$  nm. After biotinylated AChE molecules were further immobilized onto the avidin-biotin-CS-AuNPs film, the image showed the presence of the large agglomerate of AChE molecules on the modified gold surface (Fig. 3(d)) and the thickness of all the layers increased to 11 nm. The surface morphology could be clearly distinguished from that in Figure 3(c). On the base of AFM results, we conclude that AChE has been successfully immobilized on the electrode surface and thus the biosensor has been fabricated.

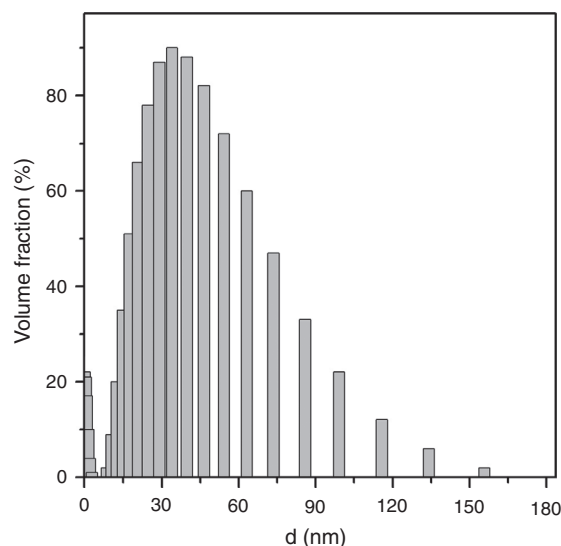


**Fig. 2.** Diameter size of gold nanoparticles.

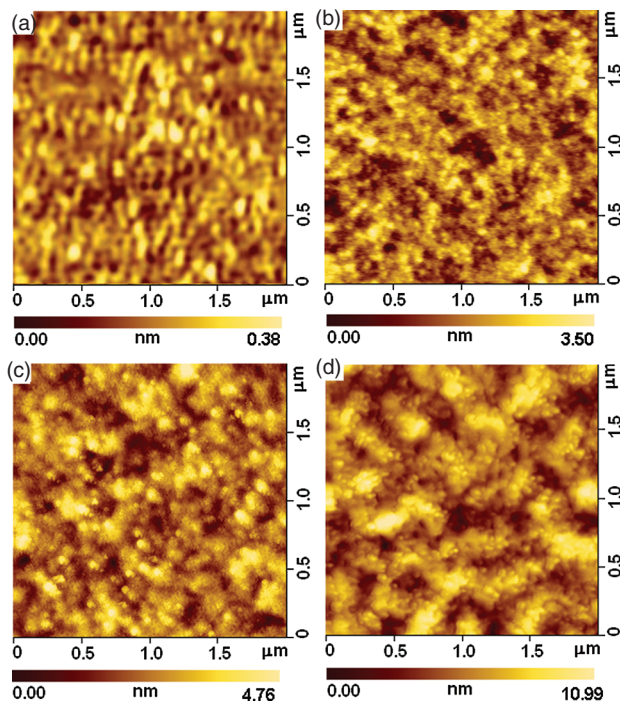


**Fig. 3.** AFM images of (a) bare Au slice, (b) biotin-CS-AuNPs deposited on Au slice, (c) avidin-biotin-CS-AuNPs on Au slice and (d) AChE-biotin-avidin-biotin-CS-AuNPs on Au slice.

### 3.4. AC Impedance Measurements

An equivalent circuit  $R_s(R_{ct} \text{ CPE})$  was used to model the impedance data (inset in Fig. 4), thus enabling the extraction of electrical parameters, such as resistance, from the impedance spectra.<sup>34</sup> As seen from the electrochemical impedance spectra, the electron transfer resistances of  $\text{Fe}(\text{CN})_6^{4-/3-}$  at bare electrode

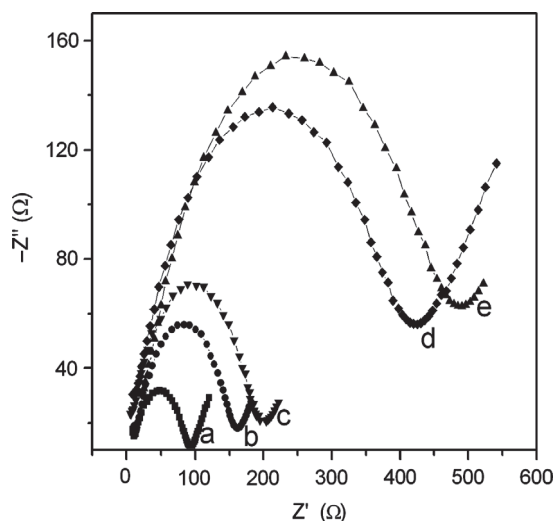


**Fig. 4.** Impedance measurements of (a) bare Au, (b) biotin-CS-AuNPs/Au, (c) avidin-biotin-CS-AuNPs/Au, (d) AChE-biotin-avidin-biotin-CS-AuNPs/Au and (e) biotin-CS/Au in 5 mM  $\text{Fe}(\text{CN})_6^{4-/3-}$ .

(curve (a)), biotin-CS-AuNPs/Au (curve (b)), avidin-biotin-CS-AuNPs/Au (curve (c)) and AChE-biotin-avidin-biotin-CS-AuNPs/Au (curve (d)) were 83  $\Omega$ , 150  $\Omega$ , 175  $\Omega$  and 411  $\Omega$ , respectively. These results showed that: (1) the interface with a biotin moiety can tailor molecular recognition events at surfaces through biotin-avidin interaction.

(2) After the formation of AChE-biotin layer, a barrier to electrochemical process was introduced. The significant change occurred at AChE-biotin-avidin-biotin-CS-AuNPs/Au might be related to the interaction between biotin-avidin.

In order to confirm the significant effect of AuNPs in the rate of electron transfer at the interface, the impedance of biotin-CS/Au was further measured to be 476  $\Omega$  (curve (e)). Comparing with that of biotin-CS-AuNPs/Au (curve (b)), the charge-transfer resistance ( $R_{ct}$ ) at the interface of biotin-CS/Au was dramatically increased. This demonstrates that AuNPs immobilized on the electrode played an important role similar to an electron-conducting tunnel, making electron transfer to the electrode surface easier. These results were further confirmed by CV measurements.

### 3.5. Monitoring Bio-Specific Interactions by SPR

SPR has emerged as a powerful tool for real-time monitoring small changes in a solid/liquid interface. As shown in Figure 5, after washing with PBS for 100 sec (curve (a)), biotin-CS-AuNPs was immobilized on gold chip. The increases of signal, curves (d) and (f) indicated the binding of avidin to biotin-CS-AuNPs/Au and the binding of AChE-biotin to biotin-avidin-biotin-CS-AuNPs, respectively. Obviously, when AChE-biotin was introduced, the

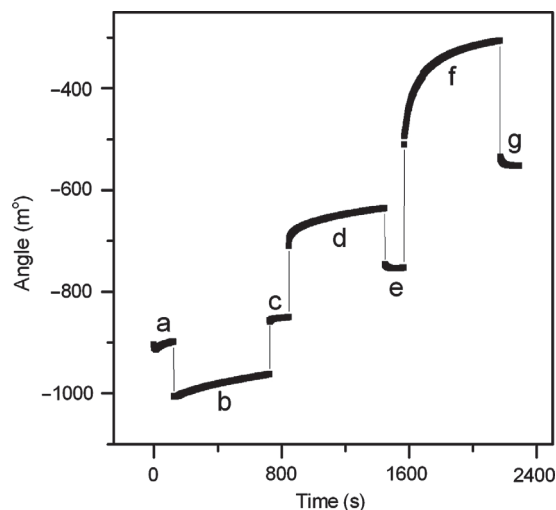


**Fig. 5.** SPR responses to sequential reaction steps between (b) biotin-CS-AuNPs and Au, (d) avidin and biotin-CS-AuNPs, (f) AChE-biotin and avidin-biotin-CS-AuNPs. Curves (a), (c), (e) and (g) are washing steps.

saturated SPR angle shift of step (f) ( $\Delta$  angle = 307 mdeg) was larger than that of step (d) ( $\Delta$  angle = 94 mdeg). From different changes of SPR angles, the binding content of AChE-biotin to avidin was 3.26-fold higher than that of avidin to biotin-CS-AuNPs. The different SPR angle shift might be related to the larger Mw of AChE. It also might be related to biotin-avidin interaction since more than one unit AChE-biotin could bind to an avidin. In order to reduce nonspecific interaction between biotin and avidin, washing steps (curve (a), (c), (e) and (g)) were carried out after every binding step.

### 3.6. Cyclic Voltammetric Behavior of AChE-Biotin-Avidin-Biotin-CS-AuNPs/Au

As shown from Figure 6, no peak was observed at avidin-biotin-CS-AuNPs/Au (curve (a)) and AChE-biotin-avidin-biotin-CS-AuNPs/Au (curve (b)) in pH 7.0 PBS. When 0.3 mM ATCl was added into PBS, the cyclic voltammograms of AChE-biotin-avidin-biotin-CS-AuNPs/Au showed an irreversible oxidation peak at 884 mV (curve (d)), while no detectable signal was observed at avidin-biotin-CS-AuNPs/Au (curve (c)). Obviously this peak came from the oxidation of thiocholine, hydrolysis product of ATCl, which was catalyzed by immobilized AChE. Thus the immobilized AChE through tailoring molecular recognition at surfaces of constructed biosensor exhibited a fast response and high affinity to its substrate. The produced current by thiocholine was used as a quantitative measurement of the enzyme activity, which could reflect the biological effect of organophosphate pesticides involved in the inhibition action.<sup>35</sup> To further demonstrate the peaks in relation to the actions of AuNPs, a comparable assay was

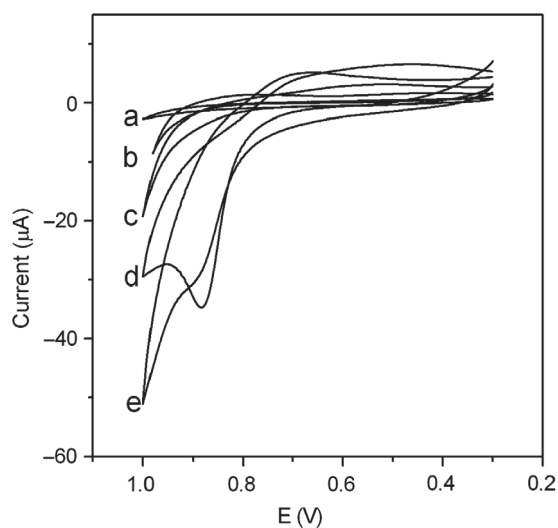


**Fig. 6.** Cyclic voltammograms of (a) bare Au, (b) AChE-avidin-biotin-CS-AuNPs/Au in 7.0 PBS, (c) avidin-biotin-CS-AuNPs/Au, (d) AChE-avidin-biotin-CS-AuNPs/Au and (e) AChE-avidin-biotin-CS/Au in pH 7.0 PBS containing 0.3 mM ATCl.

performed on AChE-biotin-avidin-biotin-CS/Au without AuNPs at the same conditions. A small oxidation peak of ATCl was seen on the AChE-biotin-avidin-biotin-CS/Au (curve (e)) and the peak potential was much higher than that on AChE-biotin-avidin-biotin-CS/Au. Apparently, a well-defined oxidation peak and negative direction-shifted oxidation potential was presented at AChE-biotin-avidin-biotin-CS/Au (curve (d)). This result indicated that the AuNPs played an important role in catalyzing the oxidative reaction of thiocholine. The surface assembling AuNPs provided a conductive pathway to electron transfer and thus promoted electron transfer reactions at a lower potential. Thus the AChE-biotin-avidin-biotin-CS-AuNPs/Au was used in following experiments.

### 3.7. Effect of Incubation Time on Response of AChE-Biotin-Avidin-Biotin-CS-AuNPs/Au

After biosensor was immersed in  $10 \mu\text{g mL}^{-1}$  dimethoate for different time, the current of ATCl decreased drastically. The decrease in peak current was related to the increase of incubation time (Fig. 7). This was because dimethoate as one of the organophosphate pesticide involved in the inhibition action to AChE, thus reduced the enzymatic activity to its substrate. Dimethoate displayed an increasing inhibition on AChE with immersing time. When the immersing time was longer than 12 min the curve tended to a stable value, indicating the binding interaction with active target groups in enzyme could reach saturation. This change tendency of peak current reflected the alteration of enzymatic activity, which resulted in the change of the interactions with its substrate. However, the maximum value of inhibition of dimethoate was not 100%, which was likely to attribute to the binding equilibrium between pesticide and binding sites in enzyme.

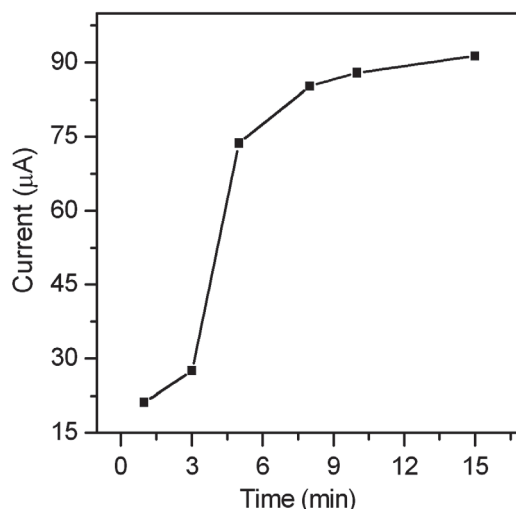


**Fig. 7.** Effect of inhibition time on amperometric response after immersion of AChE-biotin-avidin-biotin-CS-AuNPs/Au in  $10 \mu\text{g mL}^{-1}$  dimethoate solution.

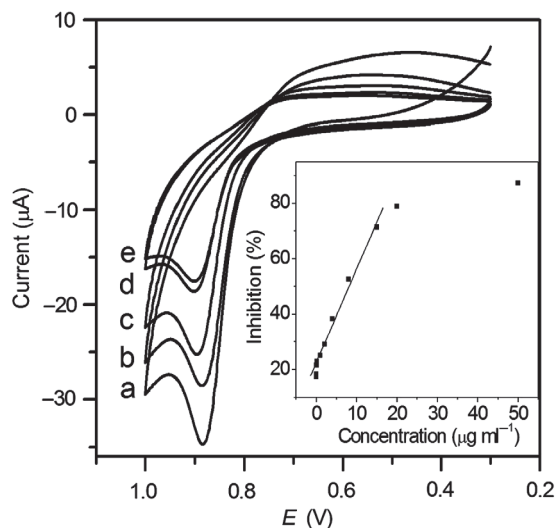


**Fig. 8.** Cyclic voltammograms of AChE-avidin-biotin-CS-AuNPs/Au in pH 7.0 PBS containing 0.3 mM ATCl after immersed in dimethoate solution with different concentrations of (a) 0, (b) 0.01, (c) 1, (d) 5 and (e) 8  $\mu\text{g mL}^{-1}$ . Inset: Calibration curve for dimethoate determinations.

### 3.8. Calibration Curve for Dimethoate Determination

Due to the notable change in voltammetric signal of the AChE-biotin-avidin-biotin-CS-AuNPs/Au, a simple method for determination of dimethoate was established. With increasing the concentrations of dimethoate the produced currents of ATCl on AChE-biotin-avidin-biotin-CS-AuNPs/Au decreased. Under the optimal experimental conditions, the inhibition of dimethoate on AChE-biotin-avidin-biotin-CS-AuNPs/Au was proportional to its concentrations in the range of 0.05 to 15  $\mu\text{g/mL}$  with the correlation coefficients of 0.9990 (Fig. 8). The detection limit was 0.001  $\mu\text{g/mL}$ .

### 3.9. Reproducibility and Stability of AChE-Biotin-Avidin-Biotin-CS-AuNPs/Au

The inter-assay precision was estimated by determining the response of 0.3 mM ATCl at five different electrodes, which were immersed in 0.1  $\mu\text{g/mL}$  and 2.0  $\mu\text{g/mL}$  dimethoate for 12 min, respectively. The coefficient of variation was calculated to be 4.6% and 2.7%, respectively, indicating acceptable fabrication reproducibility. The intra-assay precision of the sensors was evaluated by assaying one enzyme electrode for five replicate determinations, and the RSD was 3.9% at the ATCl concentration of 0.3 mM.

When the enzyme electrode was not in use, it was stored at 4 °C in dry condition. No obvious decrease in the response to ATCl was observed in the first 5-day storage. After two weeks, the sensor retains 85% of initial current response to ATCl.

## 4. CONCLUSIONS

In summary, a novel interface embedded *in situ* AuNPs and biotin in chitosan hydrogel was constructed by one-step electrochemical deposition. This deposited interface provided specific binding sites for avidin, which was further capable of attaching the AChE-biotin for biosensor design. The CV, EIS, SPR and AFM have been used as powerful tools to characterize the fabrication processes. Several advantages of the proposed method should be highlighted. First, gold nanoparticles promote electron transfer and favor the interface enzymatic hydrolysis reaction to form electroactive substance, resulting in an improvement of the detection sensitivity. Second, the immobilized AChE, as an enzyme model, showed excellent activity to its substrate and provided a quantitative measurement of organophosphate pesticide. Third, this method for biosensor design was simple, fast and “green,” which has potential application for the fabrication of amperometric biosensors. Fourth, we are currently facing the disadvantage of the low selectivity of AChE because the degree of inhibition on AChE by organophosphate pesticide is almost the same. However this does not necessarily compromise its value extended toward the preparation of other electrochemical sensors based on this mode. The ease of performance and the cost effectiveness of the system for organophosphate detection show the high potentiality in pesticide analysis.

**Acknowledgments:** The authors are gratefully acknowledging the financial support of the National Natural Science Foundation of China (No. 20705010, 30771429) and the Research Fund for the Doctoral Program of Higher Education (No. 20070511015).

## References and Notes

1. P. M. George, D. A. LaVan, J. A. Burdick, C. Y. Chen, E. Liang, and R. Langer, *Adv. Mater.* 18, 577 (2006).
2. I. J. Bruce and T. Sen, *Langmuir* 21, 7029 (2005).
3. A. Nomura, S. Shin, O. O. Mehdi, and J. M. Kauffmann, *Anal. Chem.* 76, 5498 (2004).
4. D. Du, X. Huang, J. Cai, A. D. Zhang, J. W. Ding, and S. Z. Chen, *Anal. Bioanal. Chem.* 387, 1059, (2007).
5. H. J. Kim, S. H. Choi, S. H. Oh, J. C. Woo, and I. K. Kim, *J. Nanosci. Nanotechnol.* 8, 4962 (2008).
6. J. C. Ball, L. G. Puckett, and L. G. Bachas, *Anal. Chem.* 75, 6932 (2003).
7. M. Erol, H. Du, and S. Sukhishvili, *Langmuir* 22, 11329 (2006).
8. K. V. Gujrati, R. Ashton, S. R. Bethi, S. Kate, C. J. Faulkner, G. K. Jenning, and R. S. Kane, *Langmuir* 22, 10157 (2006).
9. S. Sotiropoulou and N. A. Chaniotakis, *Anal. Chim. Acta* 530, 199 (2005).
10. V. K. Yadavalli, W. G. Koh, G. J. Lazur, and M. V. Pishko, *Sensor Actuat. B-Chem.* 97, 290 (2004).
11. G. S. Lai, H. L. Zhang, and D. Y. Han, *Sensor Actuat. B-Chem.* 129, 497 (2008).
12. Y. Han, S. Sukhishvili, H. Du, J. Cefaloni, and B. Smolinski, *J. Nanosci. Nanotechnol.* 8, 5791 (2008).

13. S. J. Lee, S. H. Jung, S. H. Lee, W. S. Han, and J. H. Jung, *J. Nanosci. Nanotechnol.* 9, 5990 (2009).
14. P. N. Deepa, M. Kanungo, G. Claycomb, P. M. A. Sherwood, and M. Collinson, *Anal. Chem.* 75, 5399 (2003).
15. H. Yi, L. Q. Wu, W. E. Bentley, R. Ghodssi, G. W. Rubloff, J. N. Culver, and G. F. Payne, *Biomacromolecules* 6, 2881 (2005).
16. L. Q. Wu, H. M. Yi, S. Li, G. W. Rubloff, W. E. Bentley, R. Ghodssi, and G. F. Payne, *Langmuir* 19, 519 (2003).
17. X. L. Luo, J. J. Xu, J. L. Wang, and H. Y. Chen, *Chem. Commun.* 16, 2169 (2005).
18. D. Du, J. W. Ding, J. Cai, and A. D. Zhang, *Colloid Surface B* 58, 145 (2007).
19. C. Kurzawa, A. Hengstenberg, and W. Schuhmann, *Anal. Chem.* 74, 355 (2002).
20. G. D. Liu and Y. H. Lin, *J. Nanosci. Nanotechnol.* 5, 1060 (2005).
21. D. Du, S. L. Liu, J. Chen, H. X. Ju, H. Z. Lian, and J. X. Li, *Biomaterials* 26, 6487 (2005).
22. L. Ding, C. Hao, Y. D. Xue, and H. X. Ju, *Biomacromolecules* 8, 1341 (2007).
23. H. Z. Huang and X. R. Yang, *Biomacromolecules* 5, 2340 (2004).
24. D. S. dos Santos, P. J. G. Oulet, Jr., N. P. W. Pieczonka, O. N. Oliveira, and R. F. Aroca, Jr., *Langmuir* 20, 10273 (2004).
25. D. Du, J. W. Ding, J. Cai, and A. D. Zhang, *J. Electroanal. Chem.* 605, 53 (2007).
26. N. Dontha, W. B. Nowall, and W. G. Kuhr, *Anal. Chem.* 69, 2619 (1997).
27. D. Du, J. W. Ding, J. Cai, and A. D. Zhang, *Sensor Actuat B-Chem.* 127, 317 (2007).
28. V. Pavlov, Y. Xiao, and I. Willner, *Nano Lett.* 5, 649 (2005).
29. D. Du, X. Huang, J. Cai, and A. D. Zhang, *Sensor Actuat B-Chem.* 127, 531 (2007).
30. X. Su, Y. J. Wu, R. Robelek, and W. Knoll, *Langmuir* 21, 348 (2005).
31. G. L. Ellman, K. D. Courtney, and V. Andres, *Biochemical Pharmacology* 7, 88 (1961).
32. X. L. Luo, J. J. Xu, Y. Du, and H. Y. Chen, *Anal. Biochem.* 334, 284 (2004).
33. G. Y. Shi, Z. Y. Sun, M. C. Liu, L. Zhang, Y. Liu, Y. H. Qu, and L. T. Jin, *Anal. Chem.* 79, 3581 (2007).
34. S. Q. Liu, K. W. Wang, D. Du, Y. M. Sun, and L. He, *Biomacromolecules* 8, 2142 (2007).
35. H. Schulze, S. Vorlov'a, F. Villatte, T. T. Bachmann, and R. D. Schmid, *Biosens. Bioelectron.* 18, 201 (2003).

Received: 12 June 2009. Accepted: 13 July 2009.

Delivered by Publishing Technology to: Purdue University Libraries  
IP: 12.170.246.82 On: Tue, 20 Oct 2015 13:14:57  
Copyright: American Scientific Publishers